Electronic Supplementary Material

Pd/Fe_3O_4 supported on bio-waste derived cellulosic-carbon as a nanocatalyst for C–C coupling and electrocatalytic application

Vishal Kandathil[1*], Akshay Moolakkil[1*], Pranav Kulkarni[1], Alaap Kumizhi Veetil[1], Manjunatha Kempasiddaiah[1], Sasidhar Balappa Somappa[2], R. Geetha Balakrishna[1], Siddappa A. Patil **(✉)**[1]

1 Centre for Nano and Material Sciences, Jain University, Jain Global Campus, Bangalore 562112, India

2 Organic Chemistry Section, Chemical Sciences & Technology Division, National Institute for Interdisciplinary Science and Technology (CSIR), Thiruvananthapuram 695019, India

E-mails: p.siddappa@jainuniversity.ac.in; patilsiddappa@gmail.com

Table of contents

Table S1. Comparison of results for the Pd/Fe_3O_4@C magnetic nanocatalyst with Pd-MNP@SCB in the Hiyama cross-coupling reaction between aryl halide and trimethoxyphenylsilane[a].

Sl No	Aryl halide	Product	Time/(min) & Yield[b]	
			$Pd/Fe_3O_4@C$	Pd-MNP@SCB
1	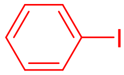	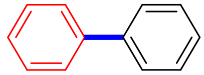	30; 95%	30; 95%
2	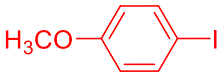	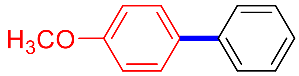	30; 90%	30; 87%
3	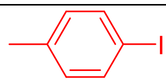	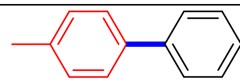	30; 90%	30; 90%
4	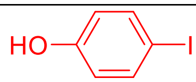	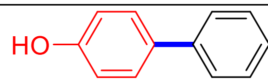	90; 70%	90; 65%
5	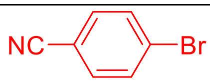	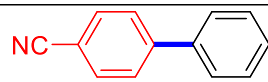	180; 80%	180; 88%

[a]Reaction conditions: Aryl halide (1 equiv.), Trimethoxyphenylsilane (1.5 equiv.), Base (3 equiv.), catalyst (0.2 mol% of Pd with respect to aryl halide) and solvent (5 mL) in air. [b]Isolated yield.

Table S2 Comparison of results for the $Pd/Fe_3O_4@C$ magnetic nanocatalyst with other catalysts in the Hiyama cross-coupling reaction between 4-bromotoluene and trimethoxyphenylsilane.

Entry	Catalyst	Solvent	Temp/ (°C)	Time/ (h)	Yield/ (%)	Ref.
1	NHC-Pd/SBA-15/IL	Dioxane:H_2O (2:1)	80	8	90	[1]
2	Pd NPs	H_2O	90	3	94	[2]
3	Pd/Fe_3O_4	H_2O	90	6	85	[3]
4	Pd nanoparticle	H_2O	90	2.5	95	[4]
5	Pd NPs	Ethylene glycol	100	1	87	[5]
6	$Pd/Fe_3O_4@C$	Ethylene glycol	100	1	92	Present work

Table S3 Comparison of results for the $Pd/Fe_3O_4@C$ magnetic nanocatalyst with other catalysts in the HER.

Entry	Catalyst	Overpotential/(mV)	Tafel Slope/ (mV/dec)	Ref.
1	f-MWCNTs@Pd/TiO_2	100	130	[6]
2	Pd/MoS_2	50	47	[7]
3	Pd NP on g-C_3N_4	55	35	[8]
4	Pd/g-C_3N_4	105	68	[9]
5	Pd/CB	117	69	[9]
6	$Pd/Fe_3O_4@C$	239	227	Present work

Analysis results of Hiyama Cross-Coupled products

1. Biphenyl (Table 2, entries 1 and 9): Colorless crystals. ^{1}H NMR (500 MHz, $CDCl_3$) δ 7.63 (d, J = 7.6 Hz, 4H), 7.48 (t, J = 7.6 Hz, 4H), 7.39 (d, J = 7.0 Hz, 2H).

2. 4-Methoxybiphenyl (Table 2, entry 2): White powder. ^1H NMR (500 MHz, $CDCl_3$) δ 7.57 – 7.52 (m, 4H), 7.42 (t, *J* = 10.6 Hz, 2H), 7.30 (t, *J* = 7.4 Hz, 1H), 7.00 – 6.96 (m, 2H), 3.85 (s, 3H).

3. 4-Methylbiphenyl (Table 2, entries 3 and 14): White crystalline solid. ^1H NMR (500 MHz, $CDCl_3$) δ 7.57 (d, *J* = 7.6 Hz, 2H), 7.49 (d, *J* = 7.3 Hz, 2H), 7.41 (t, *J* = 7.5 Hz, 2H), 7.31 (t, *J* = 7.3 Hz, 1H), 7.24 (d, *J* = 7.5 Hz, 2H), 2.39 (s, 3H).

4. 4-Hydroxybiphenyl (Table 2, entry 4): White crystals. ^1H NMR (500 MHz, $CDCl_3$) δ 7.54 (d, *J* = 7.3 Hz, 2H), 7.48 (d, *J* = 8.6 Hz, 2H), 7.41 (t, *J* = 7.7 Hz, 2H), 7.31 (d, *J* = 7.4 Hz, 1H), 6.91 (d, *J* = 8.6 Hz, 2H), 4.97 (s, 1H).

5. 2-Fluoro-1,1'-biphenyl (Table 2, entry 5): White crystals. ^1H NMR (500 MHz, $CDCl_3$) δ 7.58 (d, *J* = 7.8 Hz, 2H), 7.47 (t, *J* = 7.4 Hz, 3H), 7.40 (d, *J* = 7.2 Hz, 1H), 7.32 (d, *J* = 10.1 Hz, 1H), 7.27 – 7.14 (m, 2H).

6. 4-Cyanobiphenyl (Table 2, entry 6): Off-white crystalline powder. ^1H NMR (500 MHz, $CDCl_3$) δ 7.72 (d, *J* = 1.3 Hz, 2H), 7.69 (d, *J* = 1.4 Hz, 2H), 7.59 (d, *J* = 7.7 Hz, 1H), 7.48 (d, *J* = 6.7 Hz, 1H), 7.45 – 7.40 (m, 1H).

7. 4-Nitrobiphenyl (Table 2, entries 7 and 10): Pale yellow crystals. ^1H NMR (500 MHz, $CDCl_3$) δ 8.30 (d, *J* = 8.8 Hz, 2H), 7.74 (d, *J* = 8.8 Hz, 2H), 7.63 (d, *J* = 7.2 Hz, 2H), 7.50 (d, *J* = 8.1 Hz, 2H), 7.47 – 7.43 (m, 1H).

8. 4-Acetylbiphenyl (Table 2, entry 8): White powder. ^1H NMR (500 MHz, $CDCl_3$) δ 8.04 (d, *J* = 8.2 Hz, 2H), 7.69 (d, *J* = 8.2 Hz, 2H), 7.62 (s, 2H), 7.47 (d, *J* = 7.7 Hz, 2H), 7.41 (d, *J* = 7.1 Hz, 1H), 2.64 (s, 3H).

9. 4-Phenylbenzaldehyde (Table 2, entry 11): Yellow crystals. ^1H NMR (500 MHz, $CDCl_3$) δ 9.92 (s, 1H), 7.84 (d, *J* = 8.3 Hz, 2H), 7.41 (t, *J* = 7.5 Hz, 2H), 7.21 (d, *J* = 7.3 Hz, 1H), 7.13 – 7.01 (m, 4H).

10. 2-Phenylbenzaldehyde (Table 2, entry 12): Yellow oil. ^1H NMR (500 MHz, $CDCl_3$) δ 9.99 (s, 1H), 8.03 (d, *J* = 7.8 Hz, 1H), 7.65 (d, *J* = 1.3 Hz, 1H), 7.54 – 7.45 (m, 5H), 7.39 (d, *J* = 7.7 Hz, 2H).

11. 4-Phenylbenzoic acid (Table 2, entry 13): White solid. ^1H NMR (500 MHz, $CDCl_3$) δ 8.16 (d, *J* = 6.9 Hz, 2H), 7.70 (d, *J* = 7.0 Hz, 2H), 7.64 (d, *J* = 7.4 Hz, 2H), 7.48 (t, *J* = 6.9 Hz, 2H), 7.42 (d, *J* = 6.2 Hz, 1H).

12. [1,1'-biphenyl]-4-yl(phenyl)methanone (Table 2, entry 15): Off-white solid. ^1H NMR (500 MHz, $CDCl_3$) δ 7.92 – 7.88 (m, 2H), 7.84 (d, *J* = 8.3 Hz, 2H), 7.73 – 7.69 (m, 2H), 7.68 – 7.64 (m, 2H), 7.63 – 7.58 (m, 1H), 7.54 – 7.46 (m, 4H), 7.44 – 7.39 (m, 1H).

^1H NMR Spectra (500MHz, $CDCl_3$) of the products

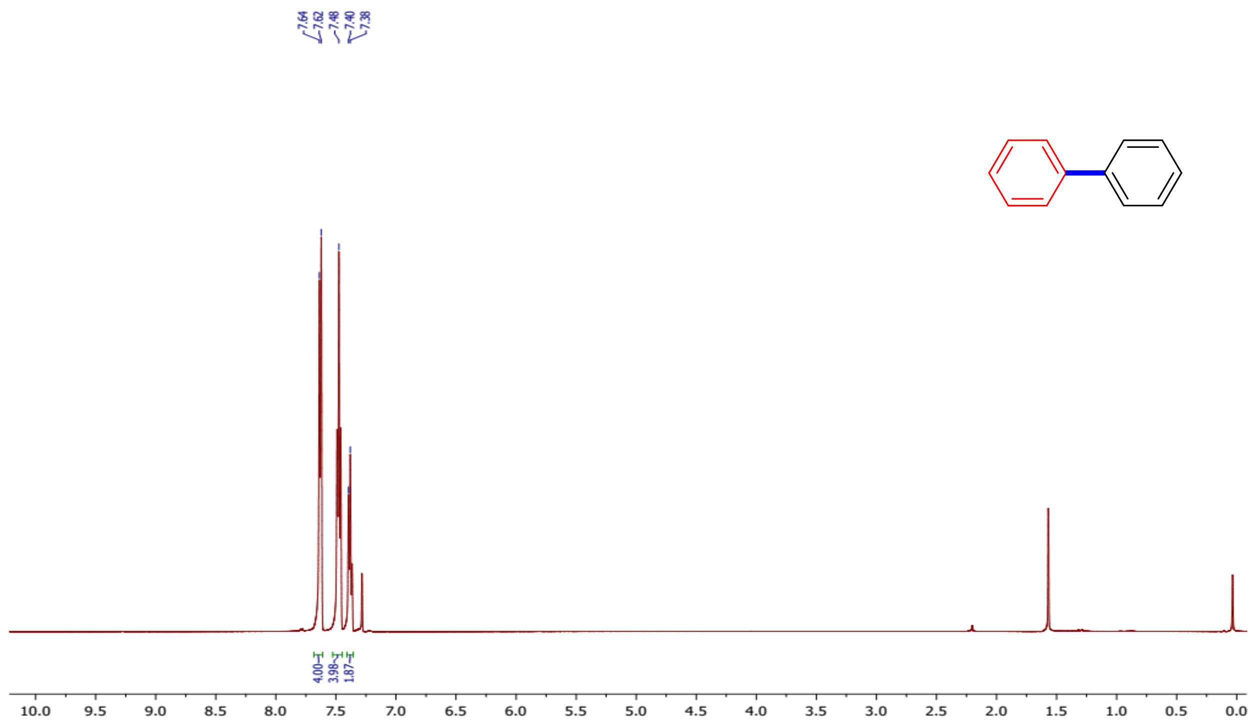
7.64
7.62
7.48
7.40
7.38
4.00
3.98
1.87
10.0 9.5 9.0 8.5 8.0 7.5 7.0 6.5 6.0 5.5 5.0 4.5 4.0 3.5 3.0 2.5 2.0 1.5 1.0 0.5 0.0

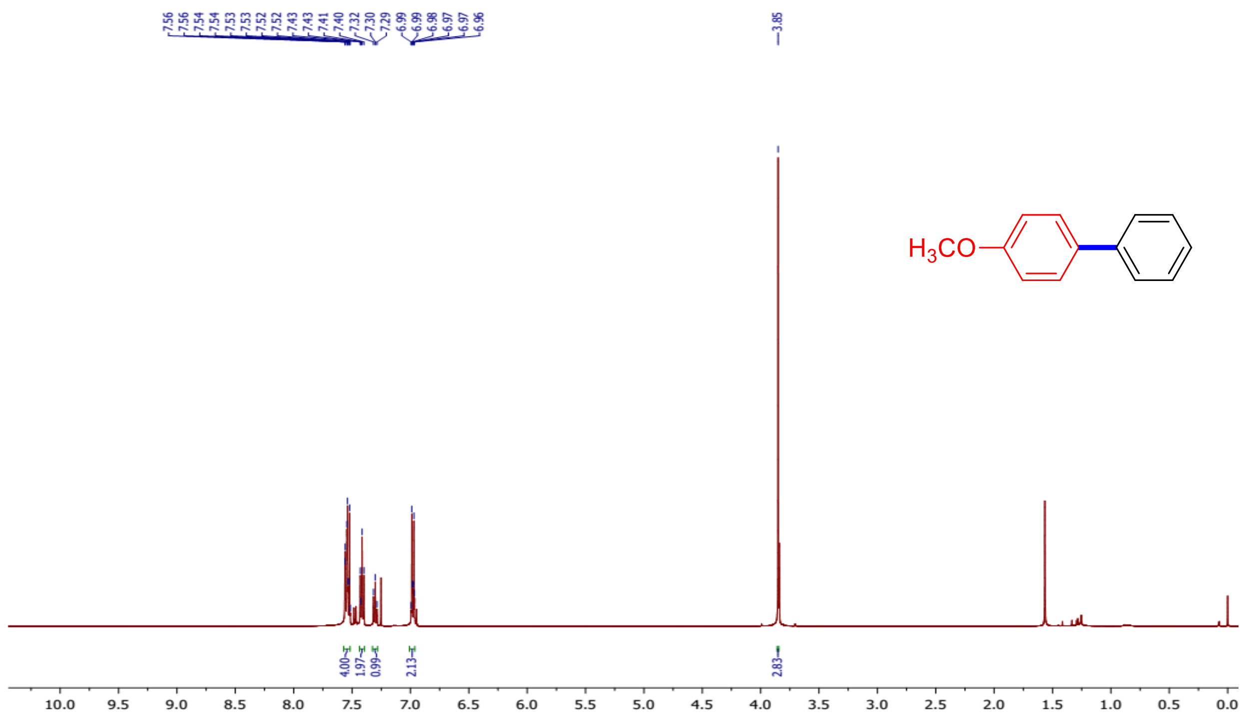
7.56
7.56
7.54
7.54
7.53
7.53
7.52
7.52
7.43
7.43
7.41
7.40
7.32
7.30
7.29
6.99
6.99
6.98
6.97
6.97
6.96
3.85
H3CO
4.00
1.97
0.99
2.13
2.83
10.0 9.5 9.0 8.5 8.0 7.5 7.0 6.5 6.0 5.5 5.0 4.5 4.0 3.5 3.0 2.5 2.0 1.5 1.0 0.5 0.0

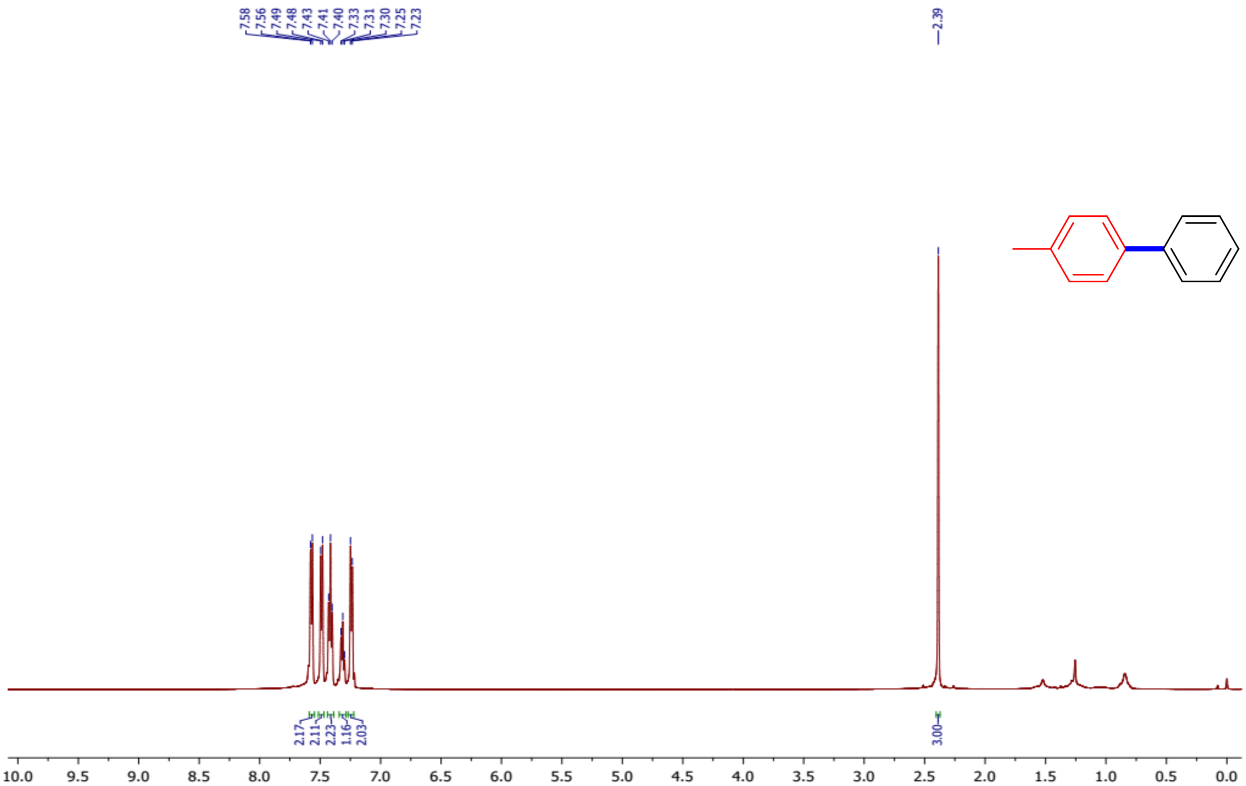
7.58
7.56
7.49
7.48
7.43
7.41
7.40
7.33
7.31
7.30
7.25
7.23
2.39
2.17
2.11
2.23
1.16
2.03
3.00
10.0 9.5 9.0 8.5 8.0 7.5 7.0 6.5 6.0 5.5 5.0 4.5 4.0 3.5 3.0 2.5 2.0 1.5 1.0 0.5 0.0

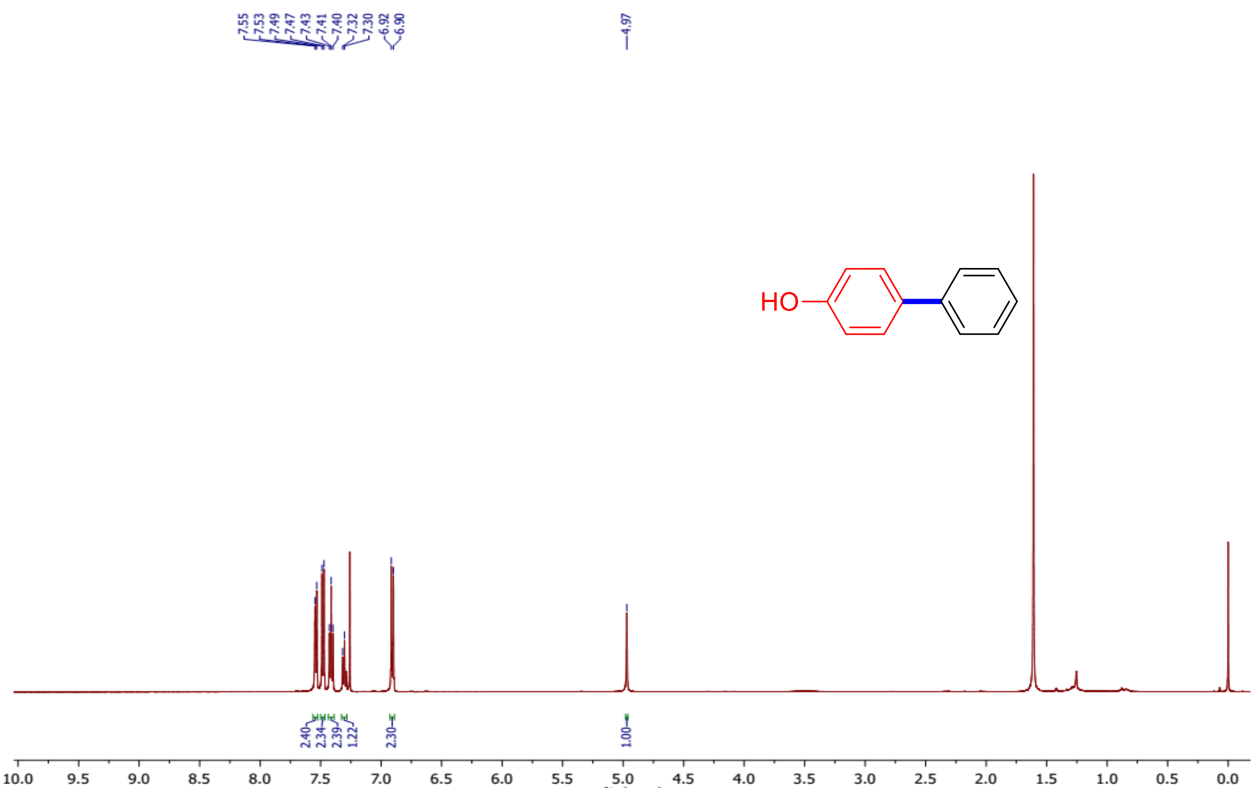
7.55
7.53
7.49
7.47
7.43
7.41
7.40
7.32
7.30
6.92
6.90
4.97
HO
2.40
2.34
2.39
1.22
2.30
1.00
10.0 9.5 9.0 8.5 8.0 7.5 7.0 6.5 6.0 5.5 5.0 4.5 4.0 3.5 3.0 2.5 2.0 1.5 1.0 0.5 0.0

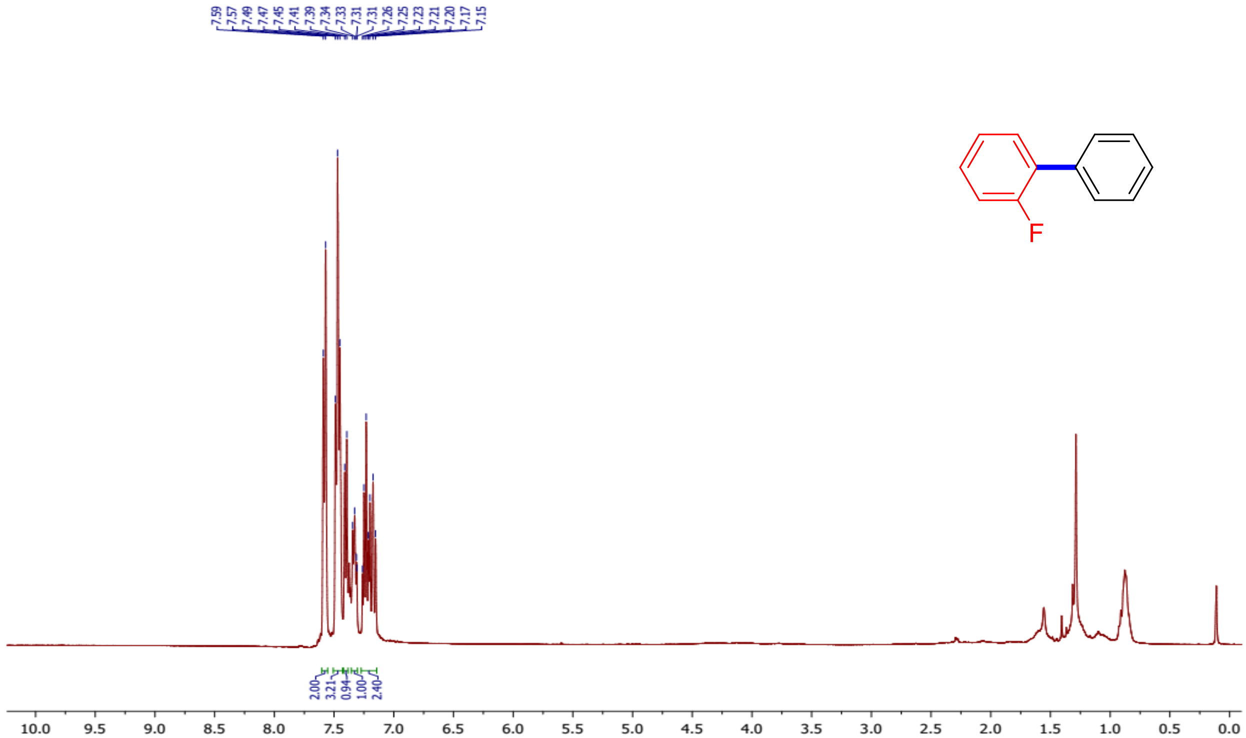
7.59 7.57 7.49 7.47 7.45 7.41 7.39 7.34 7.33 7.31 7.31 7.26 7.25 7.23 7.21 7.20 7.17 7.15
F
2.00 3.21 0.94 1.00 2.40
10.0 9.5 9.0 8.5 8.0 7.5 7.0 6.5 6.0 5.5 5.0 4.5 4.0 3.5 3.0 2.5 2.0 1.5 1.0 0.5 0.0

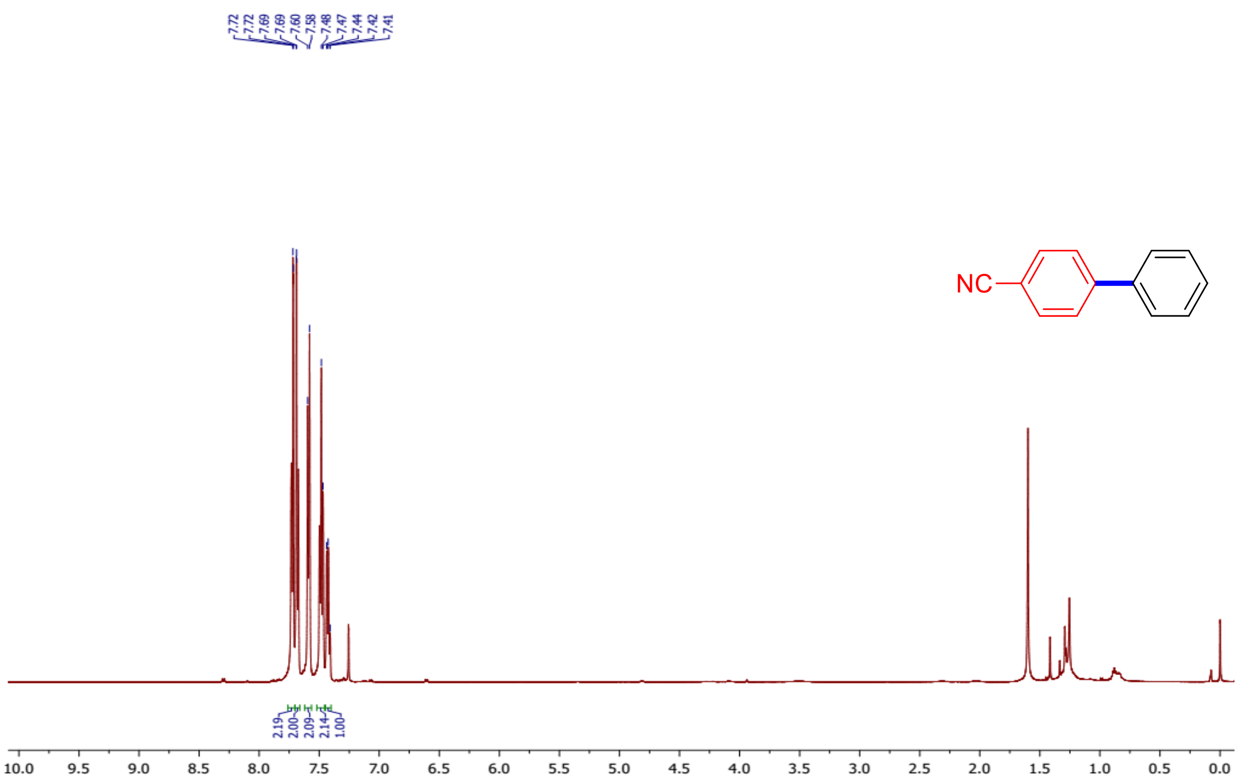
7.72 7.72 7.69 7.69 7.60 7.58 7.48 7.47 7.44 7.42 7.41
NC
2.19 2.00 2.09 2.14 1.00
10.0 9.5 9.0 8.5 8.0 7.5 7.0 6.5 6.0 5.5 5.0 4.5 4.0 3.5 3.0 2.5 2.0 1.5 1.0 0.5 0.0

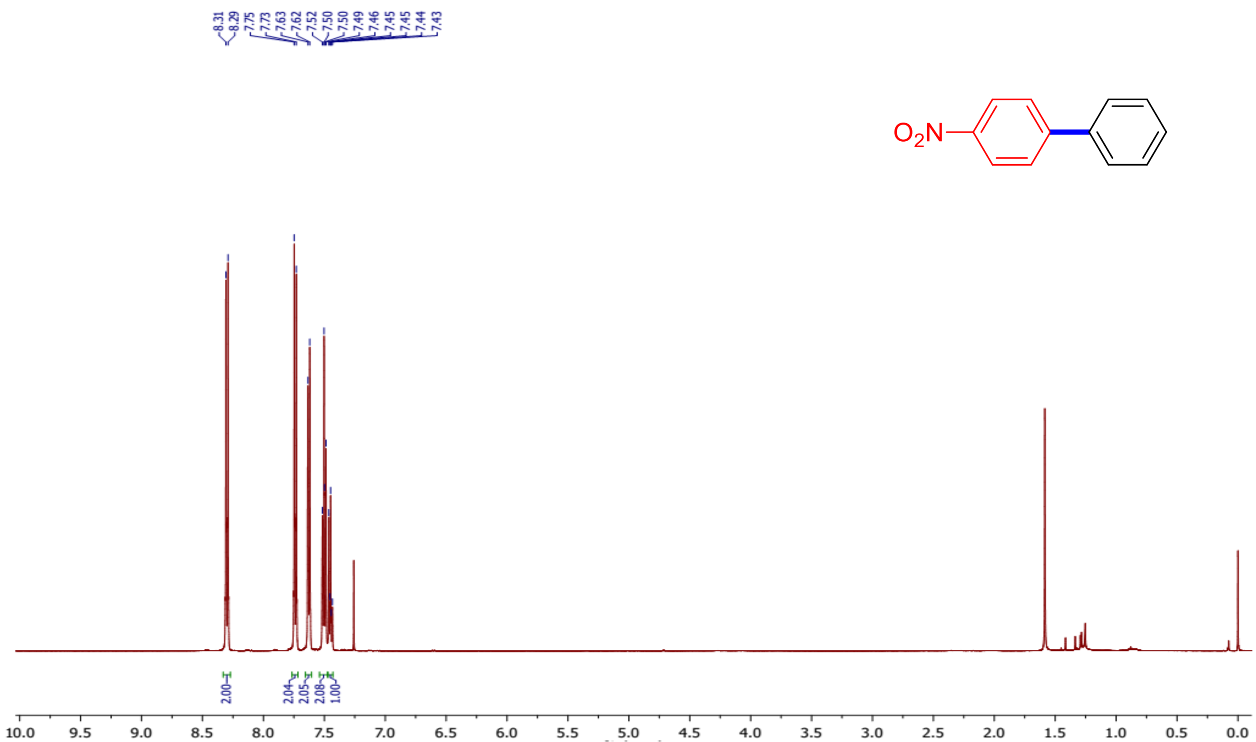
8.31
8.29
7.75
7.73
7.63
7.62
7.52
7.50
7.50
7.49
7.46
7.45
7.45
7.44
7.43
O2N
2.00
2.04
2.05
2.08
1.00
10.0 9.5 9.0 8.5 8.0 7.5 7.0 6.5 6.0 5.5 5.0 4.5 4.0 3.5 3.0 2.5 2.0 1.5 1.0 0.5 0.0

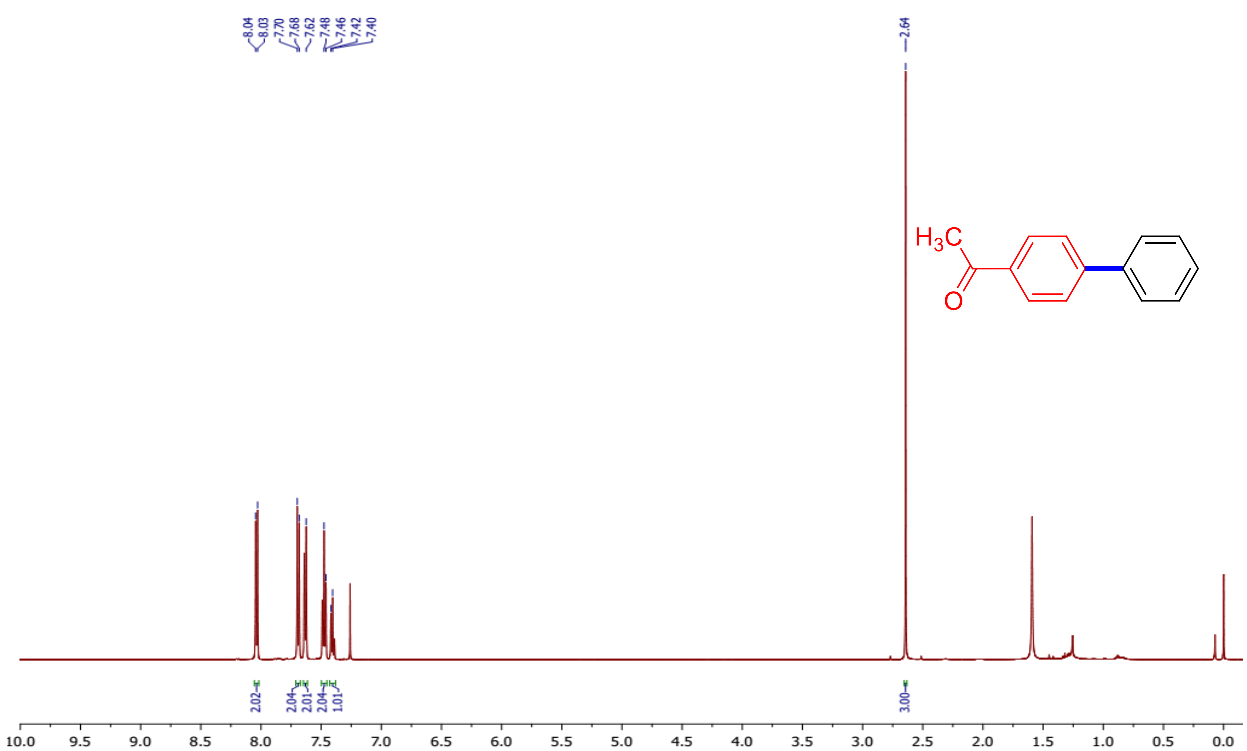
8.04
8.03
7.70
7.68
7.62
7.48
7.46
7.42
7.40
2.64
H3C
O
2.02
2.04
2.01
2.04
1.01
3.00
10.0 9.5 9.0 8.5 8.0 7.5 7.0 6.5 6.0 5.5 5.0 4.5 4.0 3.5 3.0 2.5 2.0 1.5 1.0 0.5 0.0

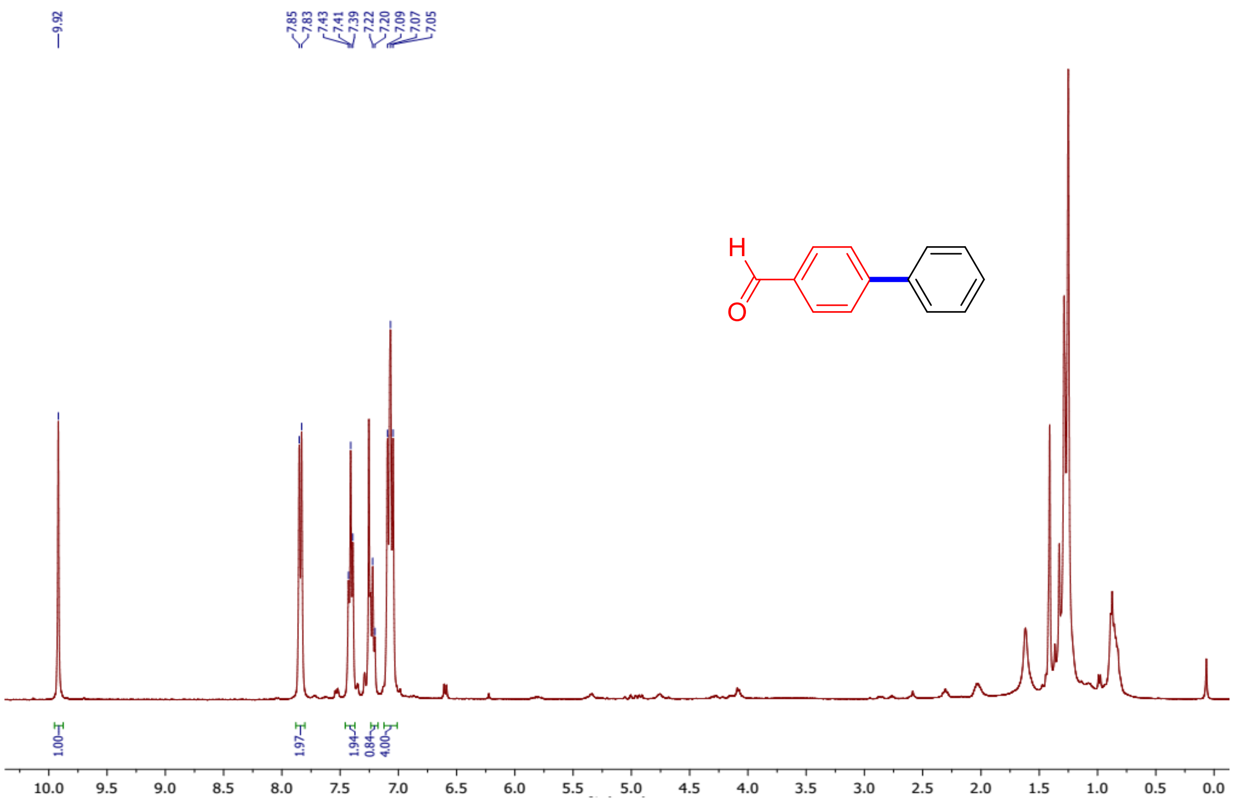
9.92
7.85
7.83
7.43
7.41
7.39
7.22
7.20
7.09
7.07
7.05
H
O
1.00
1.97
1.94
0.84
4.00
10.0 9.5 9.0 8.5 8.0 7.5 7.0 6.5 6.0 5.5 5.0 4.5 4.0 3.5 3.0 2.5 2.0 1.5 1.0 0.5 0.0

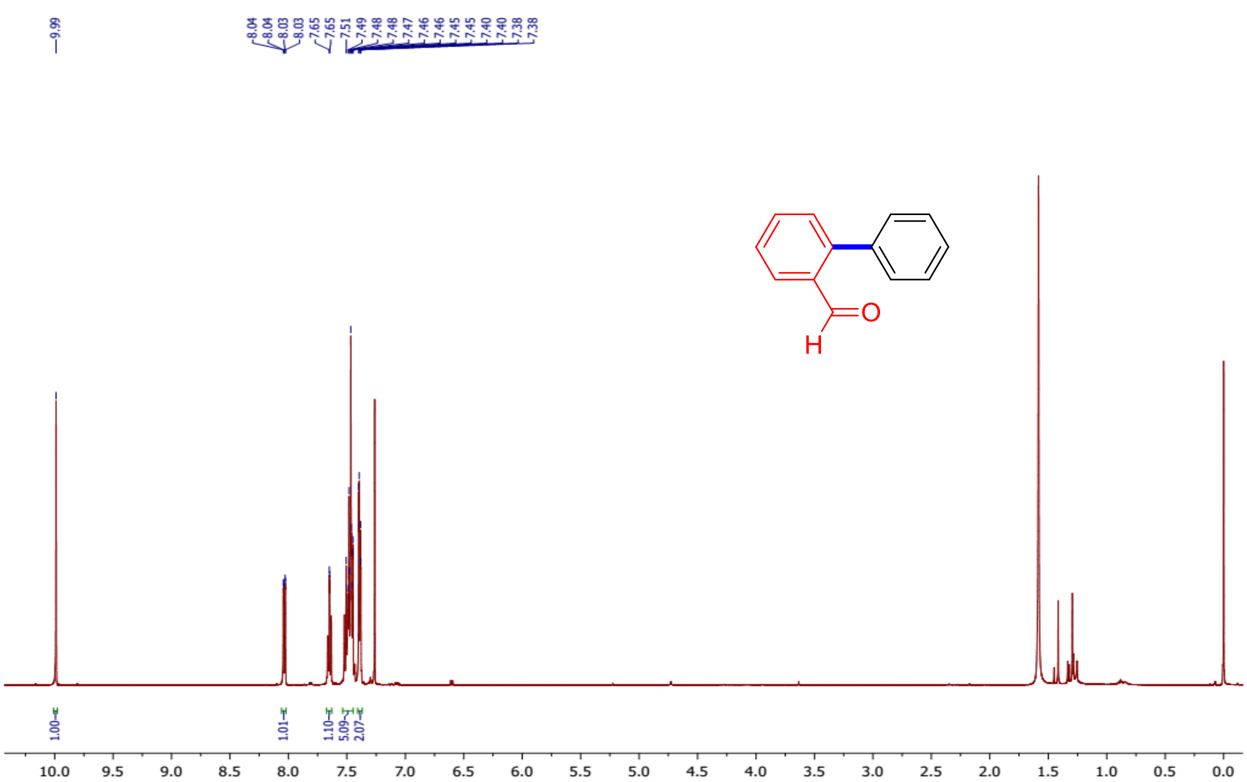
9.99
8.04
8.04
8.03
8.03
7.65
7.65
7.51
7.49
7.48
7.48
7.47
7.46
7.46
7.45
7.45
7.40
7.40
7.38
7.38
O
H
1.00
1.01
1.10
5.09
2.07
10.0 9.5 9.0 8.5 8.0 7.5 7.0 6.5 6.0 5.5 5.0 4.5 4.0 3.5 3.0 2.5 2.0 1.5 1.0 0.5 0.0

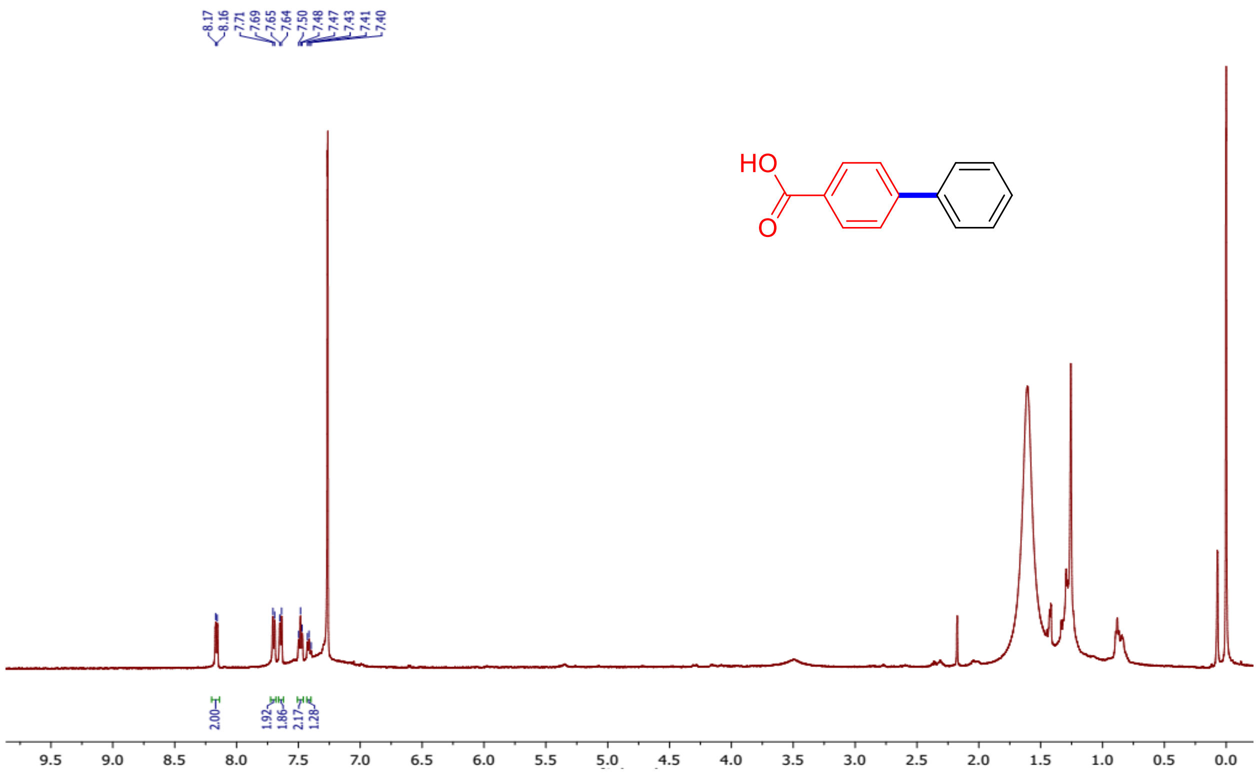
HO
O

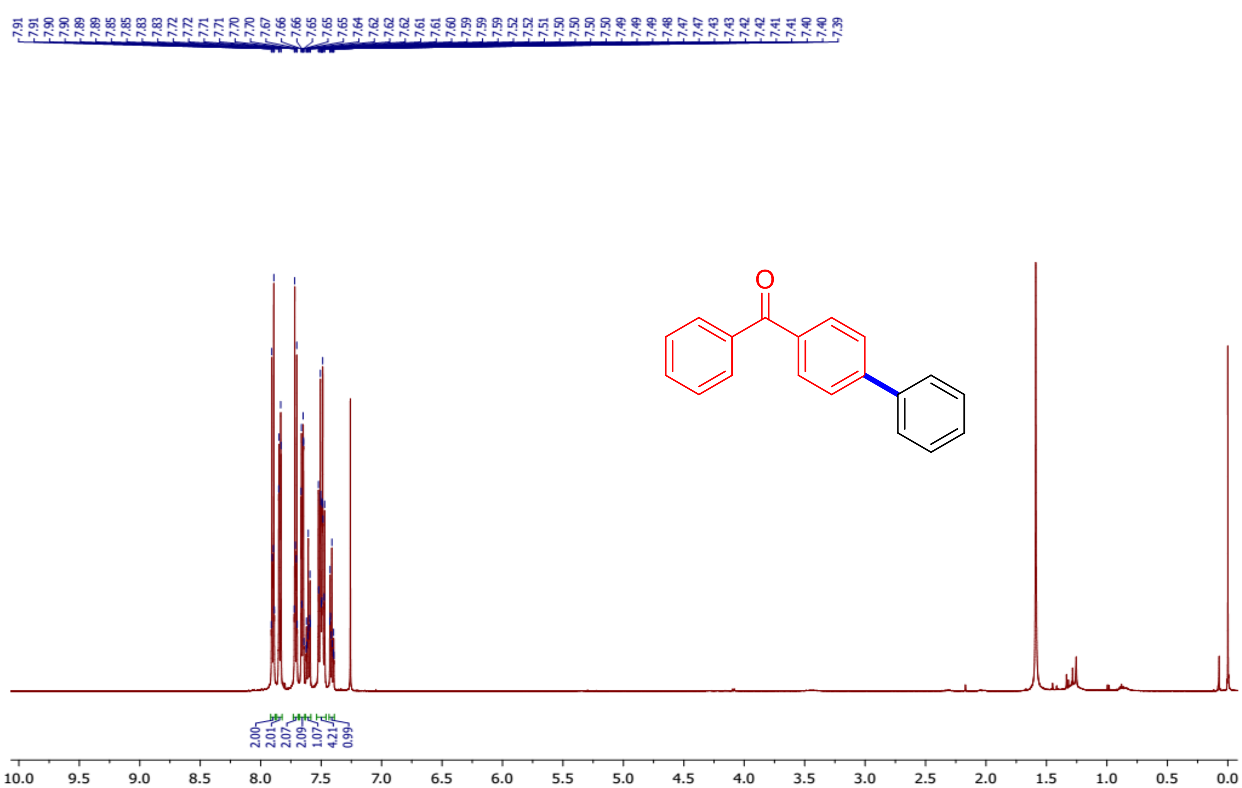
O

References

1. Rostamnia S, Hossieni H G, Doustkhah E. Homoleptic chelating N-heterocyclic carbene complexes of palladium immobilized within the pores of SBA-15/IL (NHC–Pd@ SBA-15/IL) as heterogeneous catalyst for Hiyama reaction. Journal of Organometallic Chemistry, 2015, 791: 18-23

2. Nasrollahzadeh M, Sajadi S M, Honarmand E, Maham M. Preparation of palladium nanoparticles using Euphorbia thymifolia L. leaf extract and evaluation of catalytic activity in the ligand-free Stille and Hiyama cross-coupling reactions in water. New Journal of Chemistry, 2015, 39(6): 4745-4752

3. Sreedhar B, Kumar A S, Yada D. Magnetically Recoverable Pd/Fe3O4-Catalyzed Hiyama Cross-Coupling of Aryl Bromides with Aryl Siloxanes. Synlett, 2011, 2011(08): 1081-1084

4. Srimani D, Sawoo S, Sarkar A. Convenient synthesis of palladium nanoparticles and catalysis of Hiyama coupling reaction in water. Organic Letters, 2007, 9(18): 3639-3642

5. Kandathil V, Dateer R B, Sasidhar B S, Patil S A, Patil S A. Green synthesis of palladium nanoparticles: applications in aryl halide cyanation and hiyama cross-coupling reaction under ligand free conditions. Catalysis Letters, 2018, 148(6): 1562-1578

6. Valenti G, Boni A, Melchionna M, Cargnello M, Nasi L, Bertoni G, Gorte R J, Marcaccio M, Rapino S, Bonchio M, Fornasiero P, Prato M, Paolucci F. Co-axial heterostructures integrating palladium/titanium dioxide with carbon nanotubes for efficient electrocatalytic hydrogen evolution. Nature Communications, 2016, 7(1): 1-8

7. Li B, Qiao S, Zheng X, Yang X, Cui Z, Zhu S, Li Z Y, Liang Q Y. Pd coated MoS2 nanoflowers for highly efficient hydrogen evolution reaction under irradiation. Journal of Power Sources, 2015, 284: 68-76

8. Bhowmik T, Kundu M K, Barman S. Palladium nanoparticle–graphitic carbon nitride porous synergistic catalyst for hydrogen evolution/oxidation reactions over a broad range of pH and correlation of its catalytic activity with measured hydrogen binding energy. ACS Catalysis, 2016, 6(3): 1929-1941

9. Woldetinsay M, Soreta T R, Maiyalagan T, Femi O E. Effect of support material on the electrocatalytic activity of palladium nanoparticle toward hydrogen evolution reaction. Materials Research Express, 2021, 8(2): 025501